# Optical edge detection with adjustable resolution based on liquid crystal polarization gratings

**Yang Yang (杨 阳)†, Xinyang Liu (刘新阳)†, Yan Wu (吴 艳), Ting Li (李 婷), Fan Fan (樊 帆), Huihui Huang (黄晖辉)*, and Shuangchun Wen (文双春)**

*Key Laboratory for Micro/Nano Optoelectronic Devices of Ministry of Education & Hunan Provincial Key Laboratory of Low-Dimensional Structural Physics and Devices, School of Physics and Electronics, Hunan University, Changsha 410082, China*

**Corresponding author: huangh@hnu.edu.cn*

Received March 23, 2020; accepted May 9, 2020; posted online July 20, 2020

Optical edge detection, a part of image processing, plays an important role in extracting image information used in optical analog computation. In this Letter, we raise a new way to realize optical edge detection. This design is based on two liquid crystal polarization gratings with a period of 2.2 mm, which function as a spatial differentiator. We experimentally demonstrate broadband optical detection and real-time adjustable resolution. The proposed method takes advantage of the convenience to use, simple fabrication process, and real-time tunable resolution. It may guide more significant applications in the optical field and other practical scenarios like machine vision in computers.

*Keywords: liquid crystal; polarization gratings; optical edge detection.*
*doi: 10.3788/COL202018.093501.*

With the rapid development of computer science, the development of machine vision and the Internet of Things is inseparable from digital information processing calculations. The efficiency and accuracy of converting analog signals into digital signals are important[1,2]. Optical edge detection is a basic problem in image processing and computer vision, and its purpose is to identify points with obvious brightness changes in images, especially in the feature extraction field[3–7]. Excellent optical edge detection can greatly reduce the amount of data and remove irrelevant information while retaining key image information, thus significantly improving the system efficiency and accuracy[8,9]. Up to now, so many specific edge detection methods have been proposed[10,11]. The popular methods are based on optical metamaterials and metasurfaces with their superior integration ability compared with traditional optical components[12–14]. Then, edge detection technology based on spatial differential plasma computing has emerged[15,16]. Recently, a broadband optical edge detection method based on a polarization grating (PG) metasurface structure has been implemented through experiments[17–19]. However, the fabrication processes of metasurfaces used in the above methods are very complicated or expensive[20]. At the same time, the metasurfaces with fixed parameters also limit the resolution of edge detection and cannot be flexibly applied to various application scenarios[21–23].

The liquid crystal PG can be a good substitution of spatial differentiation part in as-mentioned optical metamaterials and metasurfaces optical edge detector, and it will overcome some disadvantages[24]. Compared with crystal materials, semiconductor materials, metal materials, and metamaterials, liquid crystals have great flexibility in material design[25,26]. Through simple synthesis and mixing, the characteristics of liquid crystal materials can be controlled to a large extent. The field of optoelectronics requires devices with various characteristics, so the above characteristics from liquid crystal are extremely advantageous. Liquid crystal devices are currently attractive electronic products, and they are widely used and becoming a technology-intensive and capital-intensive high-tech industry[27–29]. Moreover, in the fabrication process, compared with traditional PGs fabrication technology, such as laser direct writing, photo-alignment technology used in the fabrication process of PGs is much simpler and more flexible. Liquid crystals have the advantage of light-controlled orientation[30], which enables free patterning by controlling the deflection angle of linearly polarized light. Thus, this liquid crystal device is suitable for large-scale production[31].

In this Letter, we propose an optical edge detection method based on two PGs. This new method not only has a simpler and cheaper way to fabricate, but can make the resolution of optical edge detection be adjustable at any time without changing the system construction. Besides, it can experimentally ensure high integration and broad-spectrum applicability.

Here, we have installed the PG with special optical properties in the $4f$ system to achieve optical edge detection. As shown in Fig. 1(a), the PG is placed at the Fourier plane of the $4f$ system. The distances between the measured object and the first lens as well as the second lens and the CCD are equal to the focal distance. The beam spot is collected by the second focus lens and then collected by the CCD. In addition, two polarizers are placed behind the measured object and in front of the CCD, playing the role of polarizer and filter, respectively. In Fig. 1(b), it can be seen that the orientation of liquid crystal

 

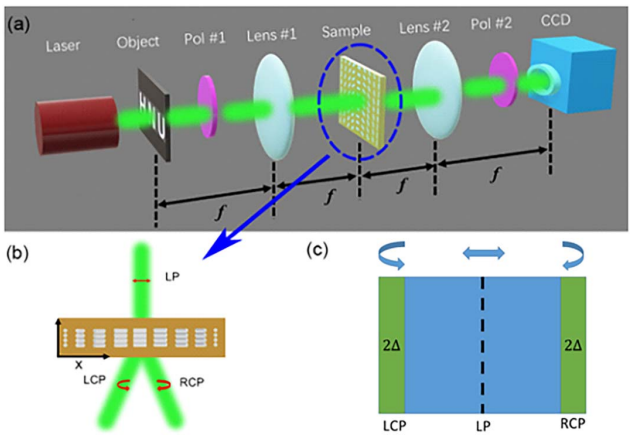


Fig. 1 (a) Experiment setup: $4f$ optical system. (b) The orientation of liquid crystal molecules in the grating films and their modulation of light. (c) Illustration of polarization dependency of PG.

molecules in the films varies along the $x$ axis periodically. When the period of PG is $\Lambda$, PG can be expressed by the Jones matrix:

$$T = R(-\Phi)\begin{bmatrix} 1 & 0 \\ 0 & \exp(-i\Gamma) \end{bmatrix} R(-\Phi). \tag{1}$$

In Eq. (1),

$$R(\Phi) = \begin{bmatrix} \cos\Phi & \sin\Phi \\ -\sin\Phi & \cos\Phi \end{bmatrix},$$
$$\Phi = \pi x/\Lambda,$$
$$\Gamma = 2\pi/\lambda(n_e - n_0)d,$$

where $T$, $\Phi$, $\Gamma$, $n_e$, and $n_0$ are the Jones matrix of the PG, PG phase gradient, phase delay of PG, ordinary and extra-ordinary refractive indices of liquid crystal birefringence[32,33]. According to the Fraunhofer formula, when the light passes through a PG, the far-field diffraction is as follows:

$$E_{\text{out}} = \frac{1}{\Lambda}\int_0^{\Lambda} T E_{\text{in}} \exp(-i2\pi m x/\Lambda)\mathrm{d}x. \tag{2}$$

When the Jones vector of incident linearly polarized light (LP) is $E_{\text{in}} = \begin{bmatrix} 1 \\ 0 \end{bmatrix}$, according to Eq. (2), the output light beam is

$$E_{\text{out}} = E_{\text{in}}(x-\Delta)\begin{bmatrix} 1 \\ -i \end{bmatrix} + E_{\text{in}}(x+\Delta)\begin{bmatrix} 1 \\ i \end{bmatrix}, \tag{3}$$

where $\Delta = \lambda\frac{f}{\Lambda}$, $\lambda$ is the working wavelength, and $f$ is the focal length. This means that the outgoing light is composed of right-handed circular polarization (RCP) and left-handed circular polarization (LCP). The LCP deviation distance is $-\Delta$, and the RCP deviation distance is $\Delta$, as shown in Fig. 1(b). When $\Delta$ is small enough compared with the outgoing spot, the two spots will overlap, as shown in Fig. 1(c). The overlapped part interferes again and becomes LP. We add polarizer 2 as an analyzer to filter out the LP[34]. Obviously, the non-overlapping part left is the edge part:

$$E_{\text{out}_{\text{edge}}} = [E_{\text{in}}(x+\Delta) - E_{\text{in}}(x-\Delta)]\begin{bmatrix} 0 \\ i \end{bmatrix}$$
$$\simeq 2\Delta\frac{\mathrm{d}E_{\text{in}}}{\mathrm{d}x}. \tag{4}$$

Therefore, LP carrying object information propagates through a PG. The LCP and RCP acquire opposite deviation distance, as indicated in Eq. (3), which manifests LCP and RCP images with $2\Delta$ shift at the image plane. The overlapped LCP and RCP components recombined to LP thus will be eliminated by the analyzer, leaving out only the edge information available for detection.

Next, a brief introduction to the production method of the measured object and PG in the experiment is given. The object to be detected in this Letter is made by three-dimensional (3D) printing. The sizes of two objects are 1 cm × 3 cm and 2 cm × 2 cm, respectively. The PG is prepared by beam interference exposure, which has a diameter $D = 2.5$ cm, as shown in Fig. 2(a). The prepared glass substrates were coated with a photo-alignment layer by the spin coating method. Then, the photo-alignment layer was irradiated with a beam produced by the interference of two LCP/RCP beams[35,36]. After exposure, liquid crystal layers were coated on top of the photo-alignment layer. In this way, we get a PG. The molecular orientation period of the film is 2.2 mm, as shown in Fig. 2(b).

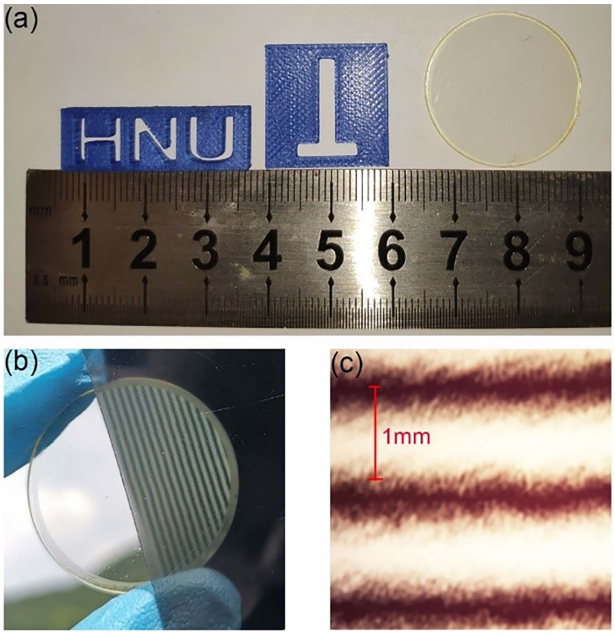


Fig. 2 (a) Physical picture of the object and the PG. (b) Visual effect of PG under natural light and linearly polarized light. (c) Image of PG under polarization microscope.

Figure 2(c) shows the image of PG under a polarization microscope. The width of the light and dark stripes corresponds to the period of the orientation change of the liquid crystal molecules[36].

First, the optical edge detection based on two PGs achieves a real-time adjustable resolution. The focal length of the lenses is 500 mm, and the illumination wavelength is 532 nm. Two PGs are superimposed on the Fourier plane of the $4f$ optical system. Two PGs liquid crystal films are placed close to each other, face to face. The combination of two PGs (CPG) can be regarded as a new type of PG[37,38], whose period will change with the angle between the CPG stripe directions[39], as shown in Figs. 3(a)–3(d). When the angle $\varphi$ of CPG increases, the period of the CPG increases. It can be known from $\Delta = \lambda \frac{f}{\Lambda}$ that the relative displacement $\Delta$ decreases as the PG period $\Lambda$ increases. The relationship between the relative displacement $\Delta$ and the parameters of CPGs (superposition angle $\varphi$ and the period $\Lambda$) is shown as Eq. (5):

$$\Delta = \frac{2f}{\cos\sqrt{1-\left(2\frac{\lambda}{\Lambda}\sin\frac{\varphi}{2}\right)^2}}. \tag{5}$$

Thus, the edge sharpness increases as the angle $\varphi$ increases. In other words, the resolution of edge detection will change with the angle between the fringe directions of the two liquid crystal PGs[38]. Figures 3(e)–3(h) show the "T" pattern without analyzer filtering. After adding the analyzer, the edge information detected by a single PG is shown in Fig. 3(i), while Figs. 3(j)–3(l) show the detection of CPG. The splitting direction of the PG is 45° to the 'T' pattern. It can be seen from the Figs. 3(i)–3(l) that there is a missing edge. The reason why we do this is that the one-dimensional optical edge detection based on liquid crystal PGs can preserve the edge to the greatest extent when detecting certain patterns. The edge widths of Figs. 3(i)–3(l) measured by CCD are 250 μm, 210 μm, 160 μm, and 100 μm. In this way, CPG achieves optical edge detection with real-time adjustable resolution. Our edge detection system adjusts resolution with simple rotations without changing components. It is worth noting that whether the combination is accurately located on the Fourier plane will greatly affect the quality of edge detection[40]. Therefore, how to make the thickness of the two superimposed PGs smaller is a direction to optimize the edge detection results. Then, we perform a broad-spectrum experiment on edge detection. The red, green, and blue light beams pass through the $4f$ system, and we obtain images without an analyzer, as shown in Figs. 4(a), 4(c), and 4(e). We put an analyzer after lens 2 so that only the edge information can go through, as displayed in Figs. 4(b), 4(d), and 4(f). It is obvious that after the beams of different wavelengths use the system clear edge information can be successfully obtained[41]. Adjusting the thickness of PGs can form ±1-order spots with higher diffraction efficiency, and zero order can be filtered by the analyzer. Therefore, different wavelengths will not affect the edge detection results. Practice has proved that edge detection based on PGs has a broad spectrum and the shorter the wavelength, the higher the resolution of edge detection. If the system works under natural light, the short-wave component should be used for edge detection in order to achieve higher resolution.

In addition, it can be found from Fig. 4 that the edge information is not a uniform edge, but a "one-dimensional edge" that is brighter in a certain direction. The deflection characteristic of the PG explains this phenomenon: the deflection directions of LCP and RCP are opposite, which means that the relative displacement of the two beams is one-dimensional. Therefore, how to optimize the beam deflection characteristics of the PG is also one of the directions to obtain better edge detection results.

In this study, CPG was combined with a $4f$ optical system to achieve optical edge detection. We experimentally prove that one of the two parallel superimposed PGs can be rotated to adjust the resolution of optical edge detection. Therefore, our optical edge detection system is suitable for a variety of edge detection scenarios without

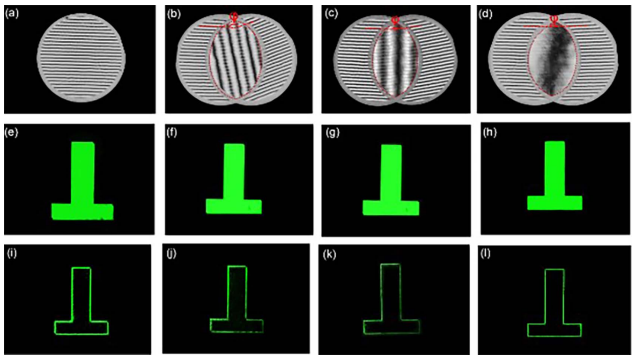


Fig. 3 (a)–(d) The effect of two liquid crystal PGs superimposed on each other. (e)–(h) Pictures of a light beam without an analyzer. (i)–(l) The edge information patterns after the filter.

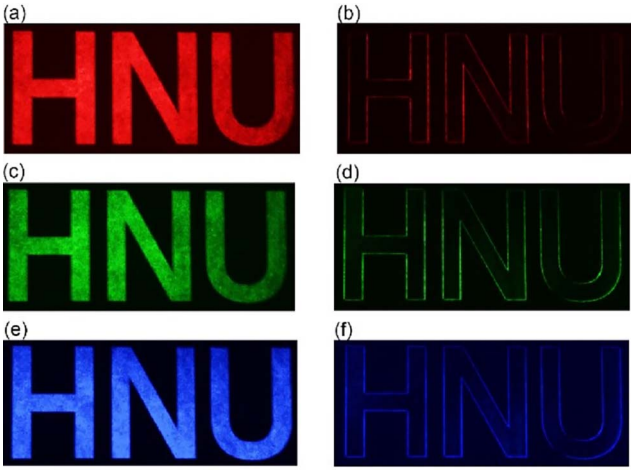


Fig. 4 (a), (c), and (e) The complete pattern of "HNU" that carries edge information without the polarizer after lens 2. (b), (d), and (f) The final edge pattern of "HNU" filtered by the polarizer and captured by CCD.

changing the system structure. Besides, we verified the broad-spectrum applicability of CPG in optical edge detection. The results show that when different wavelengths are incident, the edge information of the hollow-out pattern is still excellent. In conclusion, optical edge detection based on CPG is an effective and feasible edge detection method. The system can be applied to image processing on compact optical platforms (such as mobile phones), high-contrast microscopes, real-time object detection, and smart cameras. In the future, we plan to start with the manufacturing process and optical characteristics of liquid crystal PGs and work to achieve more optimized optical edge detection.

This work was supported by the National Natural Science Foundation of China (No. 61704053), the Natural Science Foundation of Hunan Province (No. 2017JJ3032), and the Fundamental Research Funds for the Central Universities of China.

†These authors contributed equally to this work.

## References

1. J. Canny, IEEE Trans. Pattern Anal. Mach. Intell. **PAMI-8**, 679 (1986).
2. P. Perona and J. Malik, IEEE Trans. Pattern Anal. Mach. Intell. **12**, 629 (1990).
3. D. Marmanis, K. Schindler, J. D. Wegner, S. Galliani, M. Datcu, and U. Stilla, ISPRS J. Photogramm. Remote Sens. **135**, 158 (2018).
4. H. Ren, S. Zhao, and J. Gruska, Opt. Express **26**, 5501 (2018).
5. S. He, J. Zhou, S. Chen, W. Shu, H. Luo, and S. Wen, Opt. Lett. **45**, 877 (2020).
6. P. Karimi, A. Khavasi, and S. S. Mousavi Khaleghi, Opt. Express **28**, 898 (2020).
7. L. Wan, D. Pan, S. Yang, W. Zhang, A. A. Potapov, X. Wu, W. Liu, T. Feng, and Z. Li, Opt. Lett. **45**, 2070 (2020).
8. L. De Sio, D. E. Roberts, Z. Liao, S. Nersisyan, O. Uskova, L. Wickboldt, N. Tabiryan, D. M. Steeves, and B. R. Kimball, Opt. Express **24**, 18297 (2016).
9. A. Youssefi, F. Zangeneh-Nejad, S. Abdollahramezani, and A. Khavasi, Opt. Lett. **41**, 3467 (2016).
10. D. R. Solli and B. Jalali, Nat. Photon. **9**, 704 (2015).
11. P. Genevet, F. Capasso, F. Aieta, M. Khorasaninejad, and R. Devlin, Optica **4**, 139 (2017).
12. S. Yuan, D. Xiang, X. Liu, X. Zhou, and P. Bing, Opt. Commun. **410**, 350 (2018).
13. L. Wang, L. Zou, and S. Zhao, Opt. Commun. **407**, 181 (2018).
14. A. Silva, F. Monticone, G. Castaldi, V. Galdi, A. Alù, and N. Engheta, Science **343**, 160 (2014).
15. A. Roberts, D. E. Gomez, and T. J. Davis, J. Opt. Soc. Am. A **35**, 1575 (2018).
16. T. Zhu, Y. Zhou, Y. Lou, H. Ye, M. Qiu, Z. Ruan, and S. Fan, Nat. Commun. **8**, 15391 (2017).
17. X. F. Liu, X. R. Yao, R. M. Lan, C. Wang, and G. J. Zhai, Opt. Express **23**, 33802 (2015).
18. J. Zhou, H. Qian, C. F. Chen, J. Zhao, G. Li, Q. Wu, H. Luo, S. Wen, and Z. Liu, Proc. Natl. Acad. Sci. USA **116**, 11137 (2019).
19. Y. Deng, G. Jin, and J. Zhu, Chin. Opt. Lett. **17**, 092201 (2019).
20. L. Zhang, F. Li, S. Wang, Q. Wang, K. Luan, X. Chen, X. Liu, L. Qiu, Z. Chen, J. Zhao, L. Hou, Y. Gao, and G. Jia, Chin. Opt. Lett. **16**, 102401 (2018).
21. A. Saba, M. R. Tavakol, P. Karimi-Khoozani, and A. Khavasi, IEEE Photon. Technol. Lett. **30**, 853 (2018).
22. D. A. Bykov, L. L. Doskolovich, E. A. Bezus, and V. A. Soifer, Opt. Express **22**, 25084 (2014).
23. L. L. Doskolovich, D. A. Bykov, E. A. Bezus, and V. A. Soifer, Opt. Lett. **39**, 1278 (2014).
24. A. P. M. Q. Vafa, P. Karimi, and A. Khavasi, in *2018 Fifth International Conference on Millimeter-Wave and Terahertz Technologies (MMWaTT)* (2018), p. 6.
25. W. M. Gibbons, P. J. Shannon, S.-T. Sun, and B. J. Swetlin, Nature **351**, 49 (1991).
26. R. Caputo, G. Palermo, M. Infusino, and L. D. Sio, Nanospectroscopy **1**, 40 (2015).
27. S. Furumi, M. Nakagawa, S. Y. Morino, K. Ichimura, and H. Ogasawara, Appl. Phys. Lett. **74**, 2438 (1999).
28. G. Palermo, U. Cataldi, L. D. Sio, T. Bürgi, N. Tabiryan, and C. Umeton, Appl. Phys. Lett. **109**, 191906 (2016).
29. J. Zhang, Y. Nie, Q. Fu, and Y. Peng, Chin. Opt. Lett. **17**, 052201 (2019).
30. M. Schadt, H. Seiberle, and A. Schuster, Nature **381**, 212 (1996).
31. A. Acreman, M. Kaczmarek, and G. D'Alessandro, Phys. Rev. E **90**, 012504 (2014).
32. S. Pancharatnam, Proc. Indian Acad. Sci. Sec. A **44**, 398 (1956).
33. Y. Zhou, Y. Yin, Y. Yuan, T. Lin, H. Huang, L. Yao, X. Wang, A. M. W. Tam, F. Fan, and S. Wen, Liq. Cryst. **46**, 995 (2019).
34. G. P. Crawford, J. N. Eakin, M. D. Radcliffe, A. Callan-Jones, and R. A. Pelcovits, J. Appl. Phys. **98**, 123102 (2005).
35. J. A. Davis, J. Adachi, C. R. Fernández-Pousa, and I. Moreno, Opt. Lett. **26**, 587 (2001).
36. W. Fu, Y. Zhou, Y. Yuan, T. Lin, Y. Zhou, H. Huang, F. Fan, and S. Wen, Liq. Cryst. **47**, 369 (2020).
37. P. Chen, B.-Y. Wei, W. Hu, and Y.-Q. Lu, Adv. Mater. **32**, 1903665 (2019).
38. Y. Guo, M. Jiang, C. Peng, K. Sun, O. Yaroshchuk, O. Lavrentovich, and Q.-H. Wei, Adv. Mater. **28**, 2353 (2016).
39. J. Kim and M. J. Escuti, J. Opt. Soc. Am. B **36**, D42 (2019).
40. C. Oh, J. Kim, J. Muth, S. Serati, and M. J. Escuti, IEEE Photon. Technol. Lett. **22**, 200 (2010).
41. Y. Zhou, D. Fan, S. Fan, Y. Chen, and G. Liu, Appl. Opt. **55**, 5149 (2016).